Journal of Alloys and Compounds 502 (2010) 38–42

Contents lists available at ScienceDirect

Journal of Alloys and Compounds

journal homepage: www.elsevier.com/locate/jallcom

Controlled synthesis of single-crystal $SrAl_2O_4:Eu^{2+},Dy^{3+}$ nanosheets with long-lasting phosphorescence

Ying-Feng Xu[a], De-Kun Ma[a,*], Mei-Li Guan[a], Xi-An Chen[a], Qin-Quan Pan[b], Shao-Ming Huang[a,**]

[a] Nanomaterials and Chemistry Key Laboratory, Wenzhou University, Wenzhou, Zhejiang 325027, PR China
[b] Institute of Ceramic Science, Wenzhou, Zhejiang 325027, PR China

ARTICLE INFO

Article history:
Received 13 January 2010
Received in revised form 8 April 2010
Accepted 25 April 2010
Available online 5 May 2010

Keywords:
Energy storage materials
Nanostructured materials
Optical properties
X-ray diffraction
Scanning electron microscopy

ABSTRACT

Single-crystal $SrAl_2O_4:Eu^{2+},Dy^{3+}$ nanosheets were first synthesized by a reliable two-step method. More specifically, nanosheets bundles precursors were synthesized by a facile but efficient hydrothermal route in the absence of any organic additives, catalysts, and templates, and then $SrAl_2O_4:Eu^{2+},Dy^{3+}$ nanosheets were obtained by thermally splitting the precursors. The products were characterized by multiple techniques including X-ray diffraction (XRD), field-emission scanning electron microscopy (FE-SEM), and high-resolution transmission electron microscopy (HRTEM). It was found that urea was very efficient to form nanosheets bundles precursors. The as-obtained $SrAl_2O_4:Eu^{2+},Dy^{3+}$ nanosheets showed higher photoluminescence intensity (at 516 nm), compared with commercial corresponding powders. Furthermore, the $SrAl_2O_4:Eu^{2+},Dy^{3+}$ nanosheets could sustain visible greenish-yellow light in dark places more than 16 h, suggesting potential applications in many fields.

1. Introduction

As a kind of energy-saving materials, the long-lasting phosphors can adsorb sunlight and store the energy, and then gradually release the solar energy as visible light, which lead to a long-persistent afterglow in the darkness [1,2]. These unique properties have attracted extensive interest due to their wide applications in many fields such as the dial plates of glowing watch, warning signs, automobile, ship and other instruments, escape routes, and textiles [3–6]. Among various long-lasting phosphors reported, $SrAl_2O_4:Eu^{2+},Dy^{3+}$ has attracted much attention because of its high luminescent intensity, long-lasting time, chemical stability, environmental capability. Many effective techniques have been developed to synthesize the phosphors including solid-state reaction [3], sol–gel [7], co-precipitation [8], combustion [9], and reverse microemulsion method [10]. However, the phosphors synthesized by solid-state reaction route usually possess larger size and higher hardness. In order to practical application, smaller particles must be obtained by grinding the larger phosphor particles, which can easily introduce additional defects and greatly reduce the luminescence efficiency [11]. Comparatively speaking, sol–gel, co-precipitation, combustion, and reverse microemulsion method are suitable to synthesize the phosphor with smaller sizes but often difficult to achieve well-defined morphologies. The optical properties of luminescent material not only are closely related to its native crystal structure and size but also morphology. For example, $LaPO_4$:Eu nanowires could exhibit different optical properties from corresponding nanoparticles because of shape anisotropy [12]. Therefore exploring new methods for controlled synthesis of $SrAl_2O_4:Eu^{2+},Dy^{3+}$ with well-defined morphology and studying morphology-dependent properties become a very significant subject. Recently, Cheng et al. reported a soft-template assembly and heat treatment route to obtain $SrAl_2O_4:Eu^{2+},Dy^{3+}$ nanotubes [13]. Their study showed that the emission peaks of $SrAl_2O_4:Eu^{2+},Dy^{3+}$ nanotubes blue shifted and afterglow time shortened, compared with its bulk counterpart. Chen et al. developed a CTAB-assisted solution-phase synthesis and postannealing approach to prepare necklace-like $SrAl_2O_4:Eu^{2+},Dy^{3+}$ phosphors [14]. The emission wavelength of the as-obtained phosphors also blue shifted, compared with corresponding bulk materials obtained by the high-temperature ceramic sintering. Herein we present a facile two-step method for synthesizing two-dimensional single-crystal $SrAl_2O_4:Eu^{2+},Dy^{3+}$ nanosheets, needlessly using any organic additives, templates, and catalysts. More specifically, nanosheets bundles precursors were synthesized by a facile but efficient hydrothermal route, and then $SrAl_2O_4:Eu^{2+},Dy^{3+}$ nanosheets were obtained by thermally splitting the precursors.

Nanosheets can be regarded as a new class of materials possessing features such as single-crystalline quality, well-defined chemical composition, and extremely high anisotropy with a

* Corresponding author. Tel.: +86 577 88373031; fax: +86 577 88373064.
** Corresponding author. Tel.: +86 577 88373064; fax: +86 577 88373064.
E-mail addresses: dkma@wzu.edu.cn (D.-K. Ma), smhuang@wzu.edu.cn (S.-M. Huang).

0925-8388/$ – see front matter © 2010 Elsevier B.V. All rights reserved.
doi:10.1016/j.jallcom.2010.04.186

nanoscale dimension only in the *c* axis [15]. The phosphors with nanosheet-shaped structure are quite intriguing because photoluminescence excitation energy is more effectively absorbed, ascribing to their large surface-to-volume ratios with respect to those of bulk materials. Furthermore, the morphology of nanosheets is suitable for fabricating optoelectronic devices such as electroluminescence panels, which consist of a stack of functional layers or sheets [16]. Up to now, some nanosheets-based phosphors and their photoluminescence properties have been reported such as ZnS [17], $YBO_3:Eu^{3+}$ [18], $Bi_2SrTa_2O_9$ [19], $La_{0.90}Eu_{0.05}Nb_2O_7$ [20], $Eu_{0.56}Ta_2O_7$ [21] $La_{0.90}Sm_{0.05}Nb_2O_7$ [22]. However, to the best of our knowledge, there are few reports on phosphors nanosheets with long-lasting phosphorescence. In this study, single-crystal $SrAl_2O_4:Eu^{2+},Dy^{3+}$ nanosheets with long-lasting phosphorescence were synthesized by a facile two-step method.

2. Experimental

2.1. Synthesis of nanosheets bundles precursors

In a typical procedure, 5 mmol of $Sr(NO_3)_2$, 10 mmol of $Al(NO_3)_3{\cdot}9H_2O$, and 50 mmol of $CO(NH_2)_2$ were dissolved into 80 mL of distilled water in a beaker under magnetic stirring. Then 200 μL of aqueous solution of $Eu(NO_3)_3$ (0.5 M) and 200 μL of aqueous solution of $Dy(NO_3)_3$ (0.5 M) were injected into the above solution by a microliter syringe, respectively. After the solution was stirred for 5 min, it was poured into a stainless-steel autoclave with a Teflon linear of 150 mL capability and then heated at 160 °C for 24 h. After the autoclave was cooled to room temperature, the products were separated centrifugally and washed with distilled water and absolute ethanol for several times. Finally, the white and fleecy products were dried under vacuum at 60 °C for 6 h.

2.2. Synthesis of $SrAl_2O_4:Eu^{2+},Dy^{3+}$ nanosheets

The as-obtained precursors were put in the crucible and annealed in the electric muffle furnace under a weak reducing atmosphere of active carbon at 1300 °C for 2 h.

2.3. Characterization

Powder XRD was carried out with a Bruker D8 Advance X-ray diffractometer using Cu Kα radiation (λ = 0.15418 nm) at a scanning rate of 8°/min in the 2θ range from 10 to 70°. FE-SEM images and energy-dispersive X-ray (EDX) spectroscopy were taken on a Nova NanoSEM 200 scanning electron microscope (FEI Inc.). Transmission electron microscopy (TEM) observation and selected area electronic diffraction (SAED) patterns were performed with a JEOL JEM 2010 HRTEM, using an accelerating voltage of 200 kV. Photoluminescence spectra were recorded on a Fluoromax-4 spectrofluorometer (HORIBA Jobin Yvon Inc.) equipped with a 150 W xenon lamp as the excitation source.

3. Results and discussion

The phase structure, crystallinity, and purity of the precursors and the final products were investigated by powder XRD technique. Fig. 1a and b shows XRD patterns of the precursors and the products, respectively. As can be seen from Fig. 1a, the diffraction peaks of the precursors are mainly composed of two phases, orthorhombic $SrCO_3$ (JCPDS Card 05-0418) and AlOOH (JCPDS Card 74-1895, denoted as #). After calcined at 1300 °C for 2 h, the diffraction peaks of all the precursors disappeared and transformed into those of (0 1 1), (1 2 0), (−2 1 1), (2 0 0), (2 2 1), (0 3 1), (1 3 1), (0 4 0), (2 2 2), (−2 1 3), and (−4 4 1) planes of pure monoclinic $SrAl_2O_4$ (JCPDS Card 34-0379) (Fig. 1b). Relatively strong and widened diffraction peaks suggest that the products possess good crystallinity and small sizes. The EDX spectrum was further used to determine the chemical composition of the final products. The results show that the products consist of Al, Sr, O, Eu, Dy, and C (Fig. 2). C probably comes from conductive adhesive tape for supporting the sample. According to calculational results, the ratio of Sr:Al:O:Eu:Dy is ca. 0.96:2:4:0.02:0.02, indicating that the products are $SrAl_2O_4:Eu^{2+},Dy^{3+}$ and Eu^{2+} with Dy^{3+} ions are completely doped into $SrAl_2O_4$ host matrix.

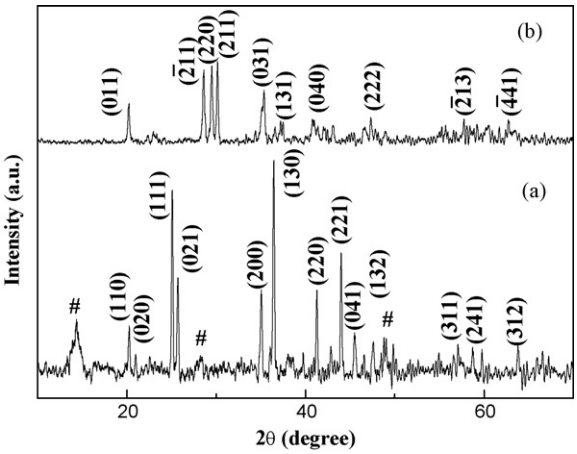

Fig. 1. Powder XRD patterns of the precursors hydrothermally synthesized at 160 °C for 24 h (a) and the final products obtained by annealing the precursors at 1300 °C for 2 h (b).

The morphologies of the precursors and the products were observed by FE-SEM, and TEM. Panels a and b of Fig. 3 show panoramic and high-magnification FE-SEM images of the precursors, respectively. The precursors consist of nanosheets bundles. Individual nanosheet has length of ca. 1 μm and width of 100 nm. The thickness of nanosheet is ca. 20 nm measured from a standing nanosheet. After heat treatment at 1300 °C for 2 h, the nanosheets bundles precursors were split and transformed into dispersed nanosheets-shaped products as shown in panels c and d of Fig. 3. It was found that the length and thickness of the products were hardly changed. But the width of the products became bigger (ca. 200 nm), compared with that of the precursors. The TEM observation on the products also indicates that nanosheet is very thin, judging from clearly visible nanosheet from the lower layer (Fig. 3e). The SAED pattern recorded on individual nanosheet consist of diffraction dots of (0 1 1), (0 1 −1), and (0 2 0) planes of monoclinic $SrAl_2O_4$, which display its single-crystal nature. The HRTEM was further used to evaluate the quality of the nanosheets. Fig. 3f shows a HRTEM image taken from the edge of individual nanosheet. No visible dislocations and defects were observed. The spacing of the adjacent lattice planes is ca. 4.45 Å, which is consistent with the interplanar spacing of (0 1 1) plane of monoclinic $SrAl_2O_4$. The HRTEM analysis shows that the as-synthesized nanosheets are well-crystallized and high-quality.

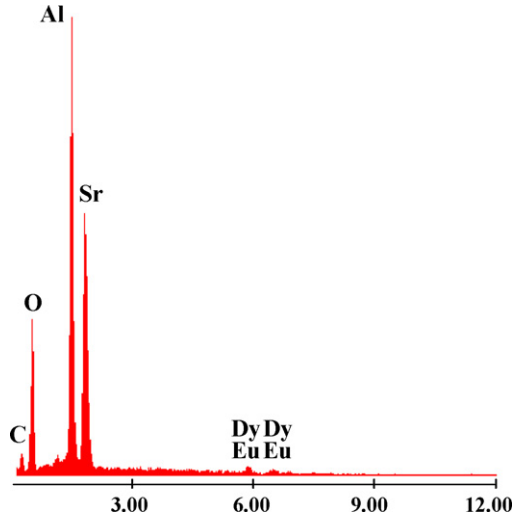

Fig. 2. EDX spectrum of the products.

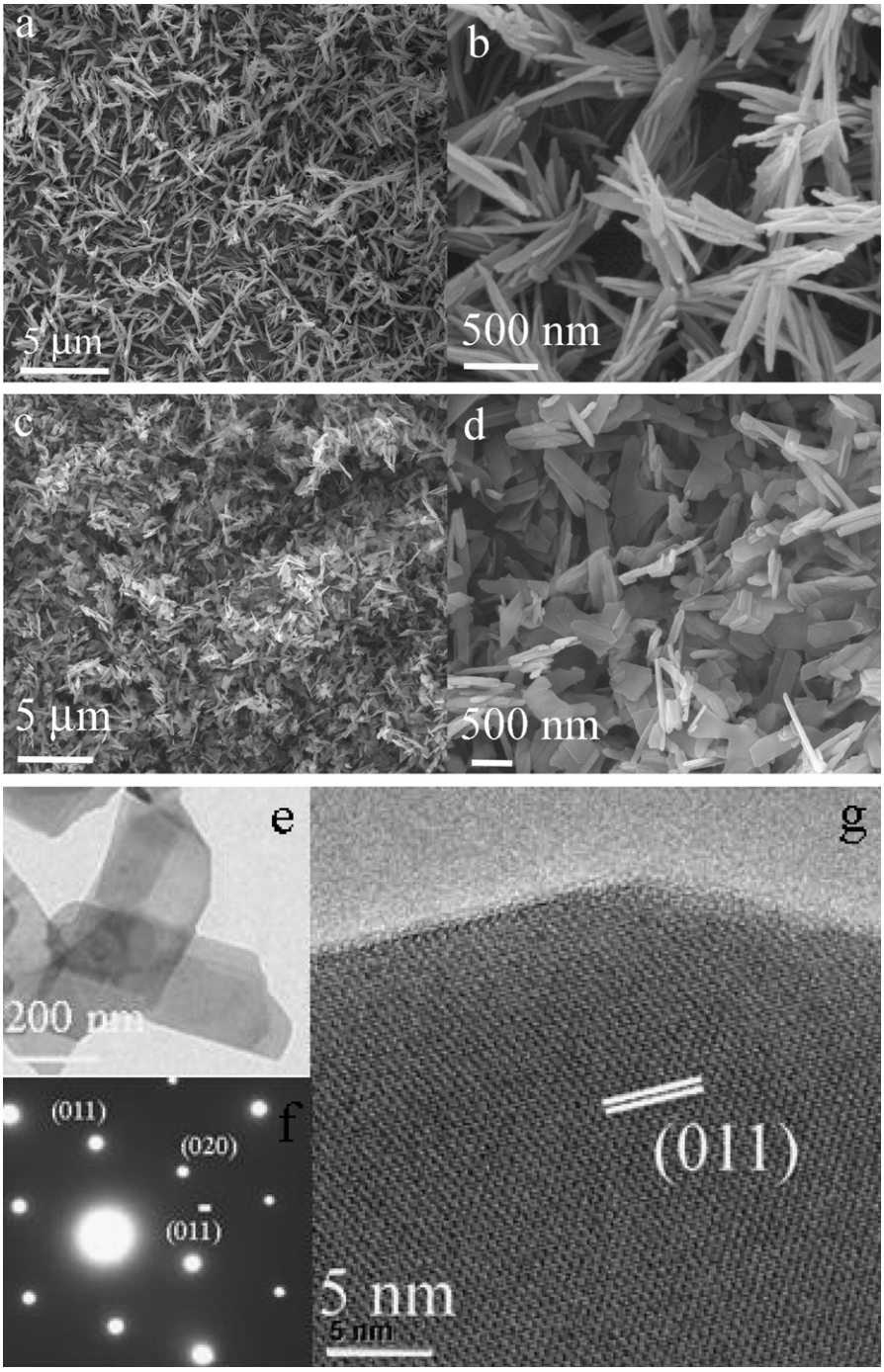

Fig. 3. (a) Panoramic FE-SEM image of the precursors. (b) High-magnification FE-SEM image of the precursors. (c) Panoramic FE-SEM image of the precursors. (d) High-magnification FE-SEM image of the products. (e) TEM image of the products. (f) SAED pattern recorded on individual nanosheet. (g) HRTEM image taken from the edge of individual nanosheet.

According to previous report [23], urea could slowly decompose into CO_2 and NH_3 in thermal aqueous solution system above 80 °C. Subsequently, the resulting CO_2 and NH_3 would dissolve in water to yield OH^- and CO_3^{2-} ions. Combined with above XRD analytical results, the main reactions for the formation of $SrAl_2O_4$ can be expressed as follows [Eqs. (1)–(6)]:

$$CO(NH_2)_2 + H_2O \rightleftharpoons CO_2 + 2NH_3 \quad (1)$$

$$CO_2 + H_2O \rightleftharpoons CO_3^{2-} + 2H^+ \quad (2)$$

$$NH_3 + H_2O \rightleftharpoons NH_4^+ + OH^- \quad (3)$$

$$Sr^{2+} + CO_3^{2-} \rightleftharpoons SrCO_3 \quad (4)$$

$$Al^{3+} + 3OH^- \rightleftharpoons AlOOH + H_2O \quad (5)$$

$$SrCO_3 + 2AlOOH \rightleftharpoons SrAl_2O_4 + CO_2 + H_2O \quad (6)$$

From Eqs. (1) to (5), it can be known that urea is necessary to produce $SrCO_3$ and AlOOH precipitations. The hydrolysis of urea is the rate control step for the formation of $SrCO_3$ and AlOOH. When urea was respectively replaced by sodium carbonate and ammonia water, keeping other conditions unchanged, only irregular and bulky precursors were obtained (Fig. 4). The hydrolysis rate of sodium carbonate and ammonia water is very fast and thus the pre-

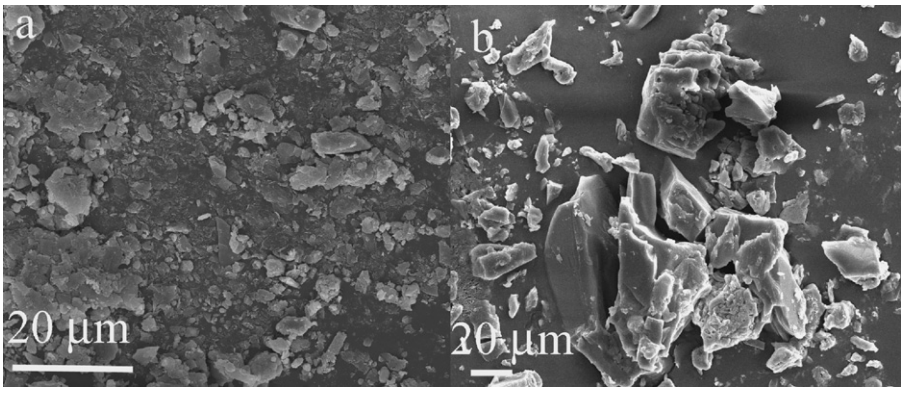

Fig. 4. FE-SEM images of the samples synthesized by respectively replacing urea with sodium carbonate (a) and ammonia water (b).

cursors precipitations will be produced immediately, which is not suitable for anisotropical growth of the crystals. Urea is more favorable to form nanosheets bundles precursors compared with sodium carbonate and ammonia, possibly ascribing to its slow hydrolysis.

Fig. 5 shows the room temperature photoluminescence excitation and emission spectra of the as-obtained $SrAl_2O_4:Eu^{2+},Dy^{3+}$ nanosheets (solid lines) and commercial $SrAl_2O_4:Eu^{2+},Dy^{3+}$ bulky powders (purchased from Jinan guangliang new materials Co. Ltd., PR China) obtained by solid-state reaction (dot lines). The excitation spectrum of $SrAl_2O_4:Eu^{2+},Dy^{3+}$ nanosheets (monitored at 516 nm) shows three obvious sub-band peaks centered at about 396, 418, and 448 nm, clearly demonstrating the crystal field splitting of five fold degenerate 5d excited level of Eu^{2+} ions. Under an excitation wavelength of 396 nm, the sample display only one greenish-yellow broad band emission peak located around 516 nm. The bandwidth of peak is quite large, ca. 200 nm, but symmetric, indicating only one luminescent center, corresponding to the $4f^6 5d^1 \rightarrow 4f^7(^8S_{7/2})$ electric dipole-allowed transition of Eu^{2+} [24]. The locations of excitation and emission peaks of $SrAl_2O_4:Eu^{2+},Dy^{3+}$ nanosheets are hardly changed, compared with commercial powders. However, the relative intensity of the excitation and emission peaks is enhanced. This point is different from previous reports on nanoparticles [24] and nanotubes of $SrAl_2O_4:Eu^{2+},Dy^{3+}$ [13]: both their emission intensity would be lowered compared with bulky $SrAl_2O_4:Eu^{2+},Dy^{3+}$. For nanosized phosphors, the adsorption of excitation light will be reduced because of strong light scattering of nanocrystals and thus their emission strength will be decreased. On the other hand, a lot of defects are easy to form on the surface of phosphors because of the high surface area of the nanometer powders prepared by general methods, which may result in the relatively less amount of luminescent centers in the host lattice available for direct radiation. Therefore it may result in the weaker fluorescence intensity. Why have the as-obtained $SrAl_2O_4:Eu^{2+},Dy^{3+}$ nanosheets stronger luminescent intensity than that of commercial bulky powders? Two main reasons can be provided at least. First, the as-synthesized $SrAl_2O_4:Eu^{2+},Dy^{3+}$ nanosheets are good crystallinity, single-crystal structure, and free of defects. Second, the photoluminescence excitation energy is more effectively absorbed by nanosheet due to its large surface-to-volume ratio with respect to those of bulk materials.

As a kind of useful long-persistent phosphorescent material, the afterglow properties of $SrAl_2O_4:Eu^{2+},Dy^{3+}$ have been extensively investigated. Its afterglow mechanism has also been understood that the electrons, captured by traps donated by Dy^{3+}, can be released slowly and recombined with the excited state of Eu^{2+} under thermal re-excitation, and then return to the Eu^{2+} ground state accompanied with light emission [3]. To the present $SrAl_2O_4:Eu^{2+},Dy^{3+}$ nanosheets, a broad phosphorescent peak centered around 516 nm can be observed after the removal of the light excitation for about 30 s, indicating that the emitting center still comes from Eu^{2+} intra-ion transition. After the phosphors were irradiated under sunlight, they could be clearly seen by the naked eye for more than 16 h in the darkness. Fig. 6 shows the decaying curves of $SrAl_2O_4:Eu^{2+},Dy^{3+}$ nanosheets and commercial counterpart at room temperature after the removal of the light excitation for about 30 s. The results indicate that the decaying processes of both the two kinds of phosphors contain

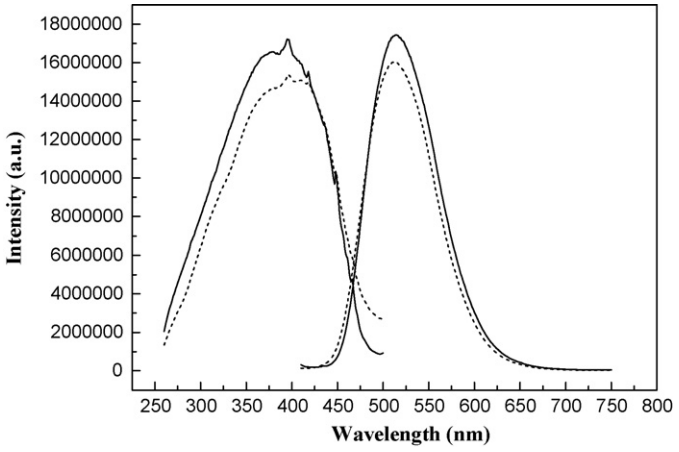

Fig. 5. Photoluminescence excitation and emission spectra of the as-obtained $SrAl_2O_4:Eu^{2+},Dy^{3+}$ nanosheets (solid lines) and commercial $SrAl_2O_4:Eu^{2+},Dy^{3+}$ powders (dot lines) at room temperature.

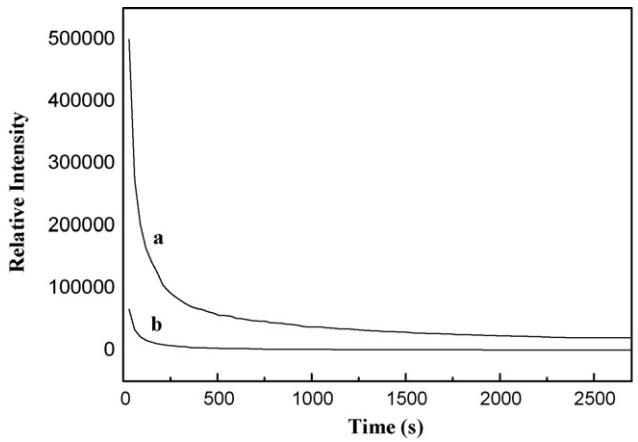

Fig. 6. Afterglow decay curves of $SrAl_2O_4:Eu^{2+},Dy^{3+}$ nanosheets (a) and commercial counterpart (b) at room temperature after the removal of the light excitation for 30 s.

a rapid-decaying process and a slow-decaying one. However, the $SrAl_2O_4$:Eu^{2+},Dy^{3+} nanosheets decayed more rapidly than commercial powders prepared by solid-state reaction. The reason may be that the as-synthesized nanosheets have good crystallinity, fewer defects in the inner phosphor, fewer crystallographic distortions, and shallower trap level than the phosphors obtained from solid-state reaction method, so that the decay of afterglow will be hastened. In addition, fast speed of hole mobility and electron–hole recombination in nanosheet with good crystallinity will decrease retraping probability and further prompt the decay process [24]. The detailed reasons need to be further clarified, and the relative study is underway.

4. Conclusions

In summary, single-crystal $SrAl_2O_4$:Eu^{2+},Dy^{3+} nanosheets have been successfully synthesized by a reliable two-step method. The nanosheets have thickness of ca. 20 nm, showing high quality. It was found that the slow hydrolysis of urea benefits the formation of nanosheets bundles precursors. The as-obtained $SrAl_2O_4$:Eu^{2+},Dy^{3+} nanosheets show higher photoluminescence intensity than commercial counterpart, which is probably attributed to high quality and nanosheet-shaped morphology. Furthermore, the present $SrAl_2O_4$:Eu^{2+},Dy^{3+} nanosheets possess long-lasting phosphorescence properties, which will have potential applications in many fields.

Acknowledgements

The authors would like to appreciate partial financial support from BSTWZ (G20070092), NSFZJ (Y4090118, R4090137), SRFZJED (Y200803419), ZJED Innovative Team, and NSFC (50772076).

References

[1] C. Chang, D. Mao, J. Shen, C. Feng, J. Alloys Comp. 348 (2003) 224–230.
[2] H.J. Song, D.H. Chen, W.J. Tang, Y.H. Peng, Displays 29 (2008) 41–44.
[3] T. Matsuzawa, Y. Aoki, N. Takeuchi, Y. Murayama, J. Electrochem. Soc. 143 (1996) 2670–2673.
[4] T. Katsumata, T. Nabae, K. Sasajima, S. Kumuro, T. Morikawa, J. Electrochem. Soc. 144 (1997) 243–244.
[5] A. Nag, T.R.N. Kutty, J. Alloys Compd. 354 (2003) 221–223.
[6] Y. Liu, C.N. Xu, J. Phys. Chem. B 107 (2003) 3991–3995.
[7] L.K. Kurihara, S.L. Suib, Chem. Mater. 5 (1993) 609–613.
[8] Y.H. Lin, Z.T. Zhang, F. Zhang, Z.L. Tang, Q.M. Chen, Mater. Chem. Phys. 65 (2000) 103–106.
[9] C.L. Zhao, D.H. Chen, Y.H. Yuan, M. Wu, Mater. Sci. Eng. B 33 (2006) 200–204.
[10] C.H. Lu, S.Y. Chen, C.H. Hsu, Mater. Sci. Eng. B 140 (2007) 218–221.
[11] R.P. Rao, J. Electrochem. Soc. 143 (1994) 189–197.
[12] L.X. Yu, H.W. Song, S.Z. Lu, Z.X. Liu, L.M. Yang, X.G. Kong, J. Phys. Chem. B 108 (2004) 16697–16702.
[13] B.C. Cheng, H.J. Liu, M. Fang, Y.H. Xiao, S.J. Lei, L.D. Zhang, Chem. Commun. 8 (2009) 944–946.
[14] X.Y. Chen, C. Ma, X.X. Li, C.W. Shi, X.L. Li, D.R. Lu, J. Phys. Chem. C 113 (2009) 2685–2689.
[15] T.G. Xu, C. Zhang, X. Shao, K. Wu, Y.F. Zhu, Adv. Funct. Mater. 16 (2006) 1599–1607.
[16] G.L. Frey, K.J. Reynolds, R.H. Friend, Adv. Mater. 14 (2002) 265–268.
[17] C.H. Liang, Y. Shimizu, T. Sasaki, H. Umehara, N. Koshizaki, J. Phys. Chem. B 108 (2004) 9728–9733.
[18] X.C. Jiang, L.D. Sun, C.H. Yan, J. Phys. Chem. B 108 (2004) 3387–3390.
[19] S. Ida, C. Ogata, U. Unal, K. Izawa, T. Inoue, O. Altuntasoglu, Y. Matsumoto, J. Am. Chem. Soc. 129 (2007) 8956–8957.
[20] T.C. Ozawa, K. Fukuda, K. Akatsuka, Y. Ebina, T. Sasaki, Chem. Mater. 19 (2007) 6575–6580.
[21] T.C. Ozawa, K. Fukuda, K. Akatsuka, Y. Ebina, T. Sasaki, K. Kurashima, K. Kosuda, J. Phys. Chem. C 112 (2008) 1312–1315.
[22] T.C. Ozawa, K. Fukuda, K. Akatsuka, Y. Ebina, K. Kurashima, T. Sasaki, J. Phys. Chem. C 113 (2009) 8735–8742.
[23] S.F. Chen, S.H. Yu, B. Yu, L. Ren, W.T. Yao, H. Cölfen, Chem. Eur. J. 10 (2004) 3050–3058.
[24] T.Y. Peng, H.P. Yang, X.L. Pu, B. Hu, Z.C. Jiang, C.H. Yan, Mater. Lett. 58 (2004) 352–356.